nature photonics

ARTICLES

PUBLISHED ONLINE: 24 JULY 2017 | DOI: 10.1038/NPHOTON.2017.116

Long-distance free-space quantum key distribution in daylight towards inter-satellite communication

Sheng-Kai Liao[1,2†], Hai-Lin Yong[1,2†], Chang Liu[1,2†], Guo-Liang Shentu[1,2†], Dong-Dong Li[1,2], Jin Lin[1,2], Hui Dai[1,2], Shuang-Qiang Zhao[3], Bo Li[1,2], Jian-Yu Guan[1,2], Wei Chen[1,2], Yun-Hong Gong[1,2], Yang Li[1,2], Ze-Hong Lin[3], Ge-Sheng Pan[1,2], Jason S. Pelc[4], M. M. Fejer[4], Wen-Zhuo Zhang[1,2], Wei-Yue Liu[3], Juan Yin[1,2], Ji-Gang Ren[1,2], Xiang-Bin Wang[2,5], Qiang Zhang[1,2,5*], Cheng-Zhi Peng[1,2*] and Jian-Wei Pan[1,2*]

In the past, long-distance free-space quantum communication experiments could only be implemented at night. During the daytime, the bright background sunlight prohibits quantum communication in transmission under conditions of high channel loss over long distances. Here, by choosing a working wavelength of 1,550 nm and developing free-space single-mode fibre-coupling technology and ultralow-noise upconversion single-photon detectors, we have overcome the noise due to sunlight and demonstrate free-space quantum key distribution over 53 km during the day. The total channel loss is ~48 dB, which is greater than the 40 dB channel loss between the satellite and ground and between low-Earth-orbit satellites. Our system thus demonstrates the feasibility of satellite-based quantum communication in daylight. Moreover, given that our working wavelength is located in the optical telecom band, our system is naturally compatible with ground fibre networks and thus represents an essential step towards a satellite-constellation-based global quantum network.

Satellite-based quantum communication has proven to be a feasible way to achieve a global-scale quantum communication network[1–9]. Very recently, a low-Earth-orbit (LEO) satellite was launched[10] for this purpose. However, with a single satellite, an inefficient 3 day period[11] is required to provide worldwide connectivity. On the other hand, similar to how the Iridium system[12] functions in classical communication, a satellite constellation (SC) composed of many quantum satellites could provide global real-time quantum communication. Such an SC is expected to operate with LEO satellites or high-Earth-orbit satellites such as geosynchronous orbit (GEO) satellites. The probability of a satellite being in the Earth shadow zone decreases rapidly with increasing orbit height (Fig. 1). A LEO satellite system has a probability of ~70% of being in the sunlight zone, whereas for a GEO satellite this rises to ~99% (ref. 13). Meanwhile, the total channel loss between a LEO satellite and the Earth and between LEO satellites is typically ~40–45 dB (refs 14,15). Therefore, to test the feasibility of an SC-based quantum network, quantum communication through a channel with at least ≥40 dB loss in daylight is essential.

There have been several pioneering experiments on daylight quantum communication before our work[16–22]. Although the experiments were novel, the maximum loss calculated from them was only ~20 dB. The main cause of the unsatisfactory performance was the strong background noise from the scattered sunlight, which was typically five orders of magnitude greater than the background noise during the night[23]. We can reduce this noise in three ways: working wavelength selection, spectrum filtering and spatial filtering.

Working wavelength selection

We first switched the working wavelength to 1,550.14 nm from the 700–900 nm used in all previous experiments. The 1,550 nm wavelength is known to be an atmospheric window. In fact, the transmission efficiency is slightly higher at 1,550 nm than at 800 nm, as shown in Fig. 1a, and from the solar spectrum in Fig. 1b we can see that the sunlight intensity at 1,550 nm is around five times weaker than it is at 800 nm. Furthermore, the main type of scattering of solar noise for links between a satellite and Earth or between two satellites is Rayleigh scattering, the intensity of which is proportional to $1/\lambda^4$. Therefore, Rayleigh scattering at 1,550 nm is only 7% of its value at 800 nm. In total, the background noise with 1,550 nm light can be reduced to 3% of the background noise of 800 nm light. We measured the noise count rate of 1,550 nm light in the daylight case by pointing a telescope at the sky to simulate satellite-to-Earth communication. The result was smaller by a factor of 22.5 than for 850 nm light. Note that all existing free-space experiments without a satellite, including this work, have been implemented on Earth, and the direction of the free-space communication is parallel to the Earth rather than pointing at the sky. In this situation, Mie scattering, which does not follow the $1/\lambda^4$ relation, will be the main noise source instead of Rayleigh scattering. Moreover, 1,550 nm is the telecom-band wavelength and is widely used for fibre-optical communication. Using the same wavelength for both free-space and fibre-optical communication is an optimal choice.

Upconversion detectors and spectral filtering

Despite the advantages of operating at 1,550 nm, researchers have been reluctant to use this wavelength due to a lack of good

[1]Shanghai Branch, National Laboratory for Physical Sciences at Microscale and Department of Modern Physics, University of Science and Technology of China, Shanghai 201315, China. [2]Synergetic Innovation Center of Quantum Information and Quantum Physics, University of Science and Technology of China, Shanghai 201315, China. [3]School of Information Science and Engineering, Ningbo University, Ningbo 315211, China. [4]Edward L. Ginzton Laboratory, Stanford University, Stanford, California 94305, USA. [5]Jinan Institute of Quantum Technology, Shandong Academy of Information and Communication Technology, Jinan 250101, China. †These authors contributed equally to this work. *e-mail: qiangzh@ustc.edu.cn; pcz@ustc.edu.cn; pan@ustc.edu.cn

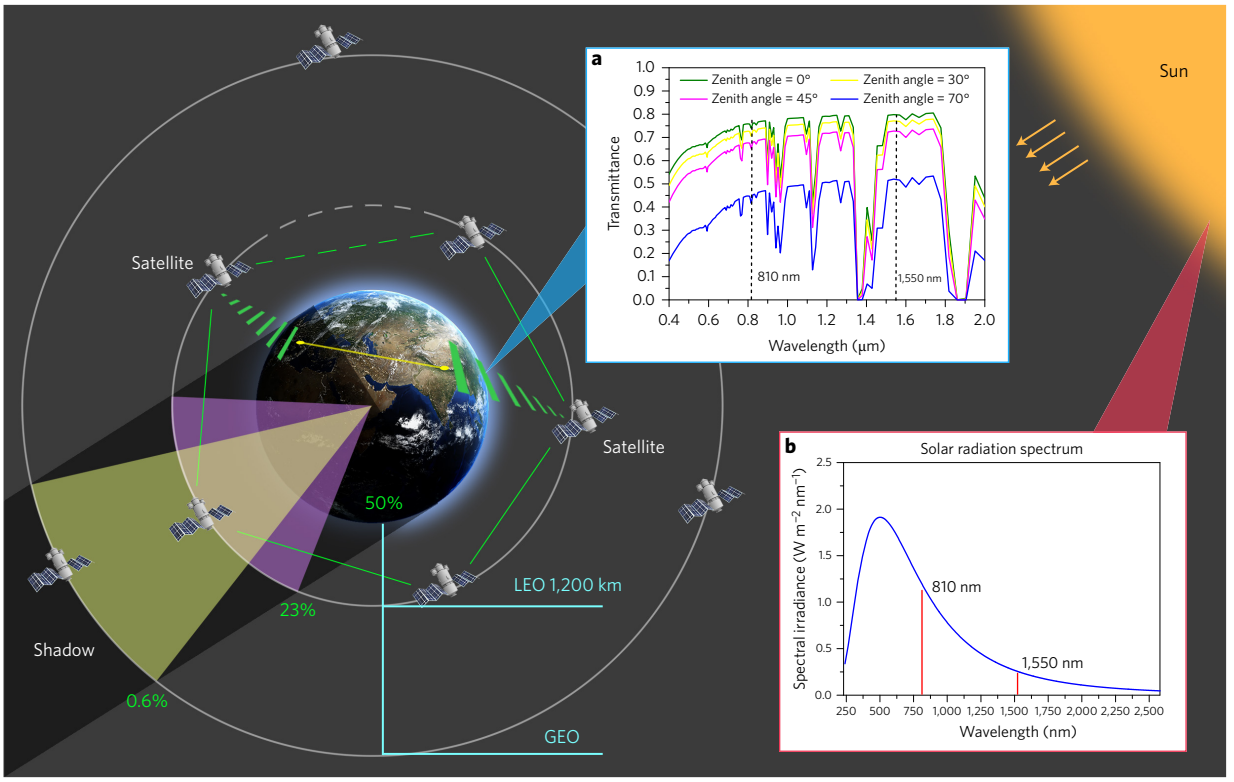

Figure 1 | Satellite-constellation-based global quantum network. A global quantum network needs many LEO satellites or several geosynchronous orbit satellites to create a satellite constellation. The time that a satellite is in the Earth shadow zone, which we call night, is inversely proportional to the orbit height of the satellite. **a**, Transmittance spectra from visible to near-infrared light in the atmosphere at selected zenith angles. **b**, Solar radiation spectrum from visible to near-infrared light.

commercial single-photon detectors for the telecom band. We have developed a compact upconversion single-photon detector (SPD)[24] (Fig. 2e). In this detector, a telecom-band photon is mixed with a strong pumping signal photon of 1,950 nm in a wavelength division multiplexing (WDM) coupler and then sent to a fibre-pigtailed periodically poled lithium niobate (PPLN) waveguide. The generated photons are collected by an anti-reflection-coated objective lens and then separated from the pump and the spurious light by a dichroic mirror (DM), a short-pass filter and a bandpass filter. A volume Bragg grating (VBG) with 95% reflection efficiency is used to further suppress the noise from both spontaneous Raman scattering generated in the nonlinear process and the sunlight background. The sum-frequency generation (SFG) photons are then collected and detected by a silicon avalanche photodiode (SAPD). Using a pump power of 200 mW, the total system detection efficiency is 8%, with an average dark count rate of ~20 Hz, which is the same as the intrinsic dark count of the SAPD.

Note that, in our experiment, the spectral bandwidth of the VBG filter is 0.05 nm (full-width at half-maximum, FWHM) at a centre wavelength tunable near 864 nm, corresponding to a bandwidth of 0.16 nm at the signal wavelength. The phase-matching condition and VBG of the detector itself realize spectrum filtering. Meanwhile, stable distributed feedback lasers (DFBs) with a 2 GHz bandwidth are used as the signal source, which guarantees that no signal will be filtered out. Such a narrowband filtering technology reduces the noise by a factor of about 100 compared with the 3–10 nm filters used in previous night experiments.

Spatial filtering with single-mode fibre coupling

To further improve the signal-to-noise ratio (SNR) we reduced the field of view (FOV) for our receiving system for spatial filtering. For free-space quantum communication at night, the FOV is usually designed to be ~100 μrad (refs 2,4,5). In most previous daylight quantum key distribution (QKD) experiments, a similarly large FOV was also used to improve the coupling efficiency at the receiver (for example, 220 μrad)[17]. However, the larger the FOV, the larger the noise introduced to the receiver. Using a single-mode fibre (SMF) to couple the signal photons is an extreme way to improve the SNR in spatial filtering, with a FOV of <10 μrad. With SMF coupling, the noise count introduced by stray light can be reduced by a factor of several hundred.

At the same time, the coupling efficiency must be maintained at a high level to make the SNR of the experiment larger. In previous experiments[25], ~0.1% SMF coupling efficiency has been achieved, which is insufficient for quantum communication. We therefore developed the SMF coupling technique further.

Unlike previous free-space experiments, which required many optical elements[6,7], we used the minimal amount of optics to design the receiving telescope and to reduce the optical attenuation and aberration. The focal length of the off-axis primary mirror was set to 2,000 mm to optimize the SMF coupling efficiency. We located only one fast-steering mirror (FSM) and one DM between the primary mirror and the SMF, and we developed an optical tracking system with 300 Hz feedback frequency to stabilize the SMF coupling (see Supplementary Information). With this set-up we could obtain a SMF coupling efficiency of >30% in the laboratory, while in the outdoor experiment the SMF coupling efficiency was reduced to 5% by horizontal air turbulence (with 3 μrad tracking precision). We emphasize that this 5% efficiency is still much higher than the 0.1% efficiency achieved in previous experiments[25]. Furthermore, in future ground-to-satellite experiments we will receive signals vertically, and the turbulence is weaker. An efficiency of 30%, similar to that obtained in the laboratory test, can be expected.

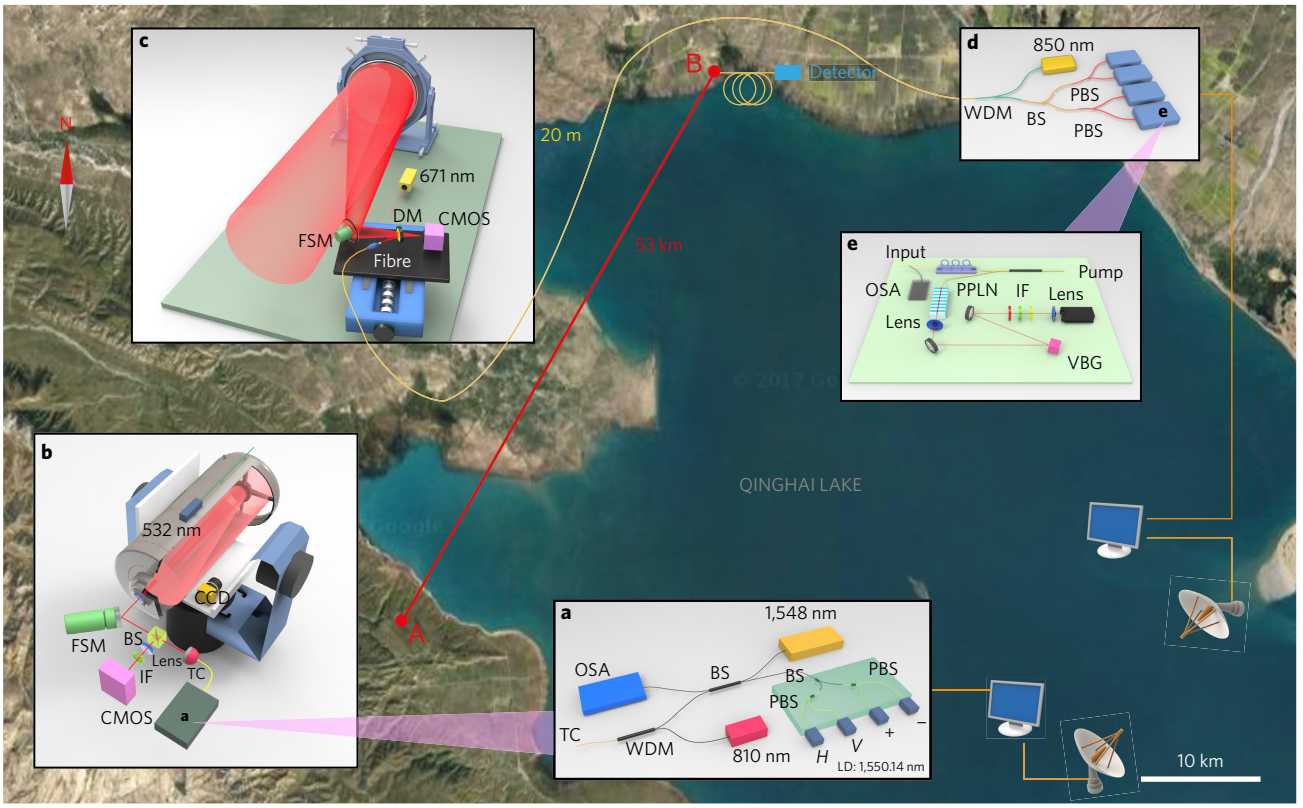

Figure 2 | Birds-eye view of the 53 km QKD experiment in daylight. Alice and Bob are located on either side of Qinghai Lake. **a**, The 1,550 nm laser diodes (LDs) are encoded to four quantum states ($|H\rangle$,$|V\rangle$,$|+\rangle$,$|-\rangle$) by two polarizing beamsplitters (PBSs) and one beamsplitter (BS). An 810 nm beacon laser and a 1,548 nm reference laser are combined and sent to a triplet collimator (TC) for optical alignment and tracking. An optical spectrum analyser (OSA) is used to calibrate the signal spectrum. WDM, wavelength division multiplexer. **b**, The sending terminal has a telescope system on a two-axis rotation stage and an optical tracking system. CCD, charge-coupled device; FSM, fast-steering mirror; IF, interference filter. **c**, The receiving terminal has an off-axial parabolic mirror and a SMF coupling module. **d**, Received photons are transmitted to the detector via a 20 m fibre. At the detection part, photons are measured with two PBSs, one BS and four detectors. **e**, Upconversion single-photon detector modules. A narrow-bandwidth volume Bragg grating (VBG) is used to narrow the working spectrum of the detectors and reduce the noise. For details of optical alignment and tracking, see Methods. PPLN, periodically poled lithium niobate. Map data: Google, CNES/Airbus, Digital Globe, Landsat/Copernicus.

Field test across Qinghai Lake

Figure 2 presents the set-up of our experiment on Qinghai Lake. We chose Qinghai Lake because it has a good visual point of view (length of 53 km). The sending terminal (Alice) was located at Heimahe village (N36°49′01.3″, E99°44′51.3″), Qinghai Province, China (Fig. 2a). Alice sent the 1,550 nm signal beam through a 53 km free-space link across Qinghai Lake to the receiving terminal (Bob), which was located at Quanji village (N37°16′42.4″, E99°52′59.9″), Qinghai Province.

At the sending terminal we developed a 1,550 nm light source with a decoy scheme[26–28]. We used four DFB lasers with a central wavelength at 1,550.14 nm and FWHM of 0.02 nm to emit 500 ps pulses. We created a standard BB84 source by combining the pulses with two polarizing beamsplitters (PBSs), one beamsplitter (BS) and one variable optical attenuator. At a clock frequency of 100 MHz, the source randomly generates one of four polarization states, $|H\rangle$, $|V\rangle$, $|+\rangle$ and $|-\rangle$, with one of three average photon numbers per pulse (0.6, 0.14, 0). Here $|H\rangle/|V\rangle$ represents horizontal and vertical polarization, $|+\rangle = (|H\rangle + |V\rangle)/\sqrt{2}$ and $|-\rangle = (|H\rangle - |V\rangle)/\sqrt{2}$. The intensity of the signal state was 0.6 per pulse. We used two decoy states: the vacuum state and a state with average photon number 0.14. The probability ratio of the signal and the two decoy states was 2:1:1. All random control signals were generated at high speed by a random number generator. The signal was then coupled into the SMF and collimated out into free space with a triplet collimator (TC) and then sent to the telescope (mounted on a two-dimensional platform, Fig. 2b). We minimized the sending divergence angle of the 1,550 nm beam to reduce geometric loss. We chose a Schmidt–Cassegrain system with a $d =$ 254 mm primary mirror for sending, because the divergence angle is proportional to the wavelength and inversely proportional to the size of the primary mirror. The measured divergence angle was 12 μrad, which is very close to the diffraction limit and four times smaller than our previous sending system[6].

At the receiving terminal, the signal light was collected by a receiving telescope (Fig. 2c), which consisted of a primary parabolic mirror with a diameter of 420 mm and focal length of 2,000 mm and a SMF coupling module with an optical tracking system (see Methods). The signal photons went through a 20-m-long SMF to the detection system. A fibre BS was used to select a measurement basis, and two fibre PBSs together with four upconversion SPDs were used for detection (Fig. 2d). All detected signals were sent into a time-to-digital converter (TDC) for analysis. The time window was set to 1 ns, for timely filtering of the noise as in previous experiments[17,19]. We also developed an efficient self-synchronized system based only on GPS, which could use fewer resources than previous pulsed-laser synchronization systems[4].

In our QKD experiment, Alice and Bob extracted the final secure key out of the raw data following a standard decoy BB84 post-processing procedure[27–29]. The final key rate formula is

$$R_{\text{pulse}} \geq qp_{\mu}\{-Q_{\mu}f(E_{\mu})H_2(E_{\mu}) + Q_1[1 - H_2(e_1)]\} \qquad (1)$$

Table 1 | Experimental parameters and results.

T (s)	Q_μ	Q_v	Y_0	E_μ (%)	E_v (%)	R_{pulse}	R_{total} (bits)
643	1.36×10^{-5}	3.99×10^{-6}	7.24×10^{-7}	3.19	9.18	9.42×10^{-7}	60,567
649	9.12×10^{-6}	2.59×10^{-6}	3.02×10^{-7}	3.24	9.49	4.27×10^{-7}	27,700
464	1.63×10^{-5}	4.11×10^{-6}	2.38×10^{-7}	1.65	3.35	1.49×10^{-6}	68,912

T is the effective time for QKD. Q_μ and Q_v are the gains for the signal states and decoy states, respectively. Y_0 is the yield for vacuum states. E_μ and E_v are the quantum bit error rate (QBER) of the signal states and decoy states, respectively. R_{pulse} is final key rate per clock cycle and R_{total} is the total final key size of the experiment.

where $q = 1/2$ is the basis reconciliation factor, p_μ is the probability of emitting signal states, Q_μ and E_μ are the gain and error rate of the signal states, respectively, and f is the error correction efficiency. The low-density parity-check (LDPC) code was used for error correction, with $H_2(e) = -e\log_2(e) - (1-e)\log_2(1-e)$ being the binary Shannon entropy function and Q_1 (e_1) the gain (phase error rate) when the source generates single-photon states. We carried out and repeated QKD experiments from 15:30 to 17:00 local time for several sunny days. Three typical groups of results are listed in Table 1. We obtained 157,179 bits during 1,756 s effective time. The final key rate was 20–400 bits per second. The variation of the final key rate was mainly due to channel loss changes in the atmospheric environment.

All the data were collected in good weather, as was the case for the long-distance QKD experiments in refs 2–4 and 6. Unfortunately, implementing quantum communication in bad weather is not possible with current technology. However, we note that there will be no turbulence or bad weather between satellites. Only when considering quantum communication between a satellite and the ground must bad weather be taken into account.

The internal modulation of the decoy/signal states guaranteed our system security against photon number splitting[30,31] and unambiguous-state-discrimination attack[32]. The total loss over our 53 km free-space QKD was 48 dB, which consisted of a 14 dB SMF coupling loss and 34 dB other loss (including geometric loss, air attenuation, receiving loss and detection loss). Our experiment showed the success of QKD through a 48 dB loss channel, which offers strong support for an SC-based quantum network.

In our experiment, both the sender and receiver are fixed and, in general, a full simulation of SC quantum communication should include a fast-moving party. However, in our previous study[6] we developed high-precision acquisition, tracking and pointing (ATP) technology and implement QKD with a fast-moving platform. Also, SMF coupling technology for LEO–ground[33] and GEO–ground[34] have been well verified. We believe that with the ATP technology developed in previous experiments, our work provides solid proof of SC-based quantum communication.

Conclusion

We have successfully demonstrated free-space QKD over 53 km in daylight. With a working wavelength of 1,550 nm, upconversion SPD and SMF coupling, we offer a solution to the problem of quantum communication in daylight. Our work proves the feasibility of a LEO quantum SC that works predominantly in daylight. Moreover, our work also offers an optimal option for a global quantum network consisting of a quantum SC and existing ground fibre networks. Our free-space single-mode coupling technology is also very useful for both free-space quantum communication and laser communication applications such as QKD with imperfect devices[35,36], quantum teleportation[37], quantum repeaters[38] and quantum metrology[39,40]. Moreover, the SC-based quantum network can also find rapid application in precisely sharing timing information globally[41].

The communication distance and secure key rate still have room for improvement. The system repetition rate can be improved by increasing the upconversion detector rate, which may become as large as 2 GHz (ref. 42). With cavity-enhanced SAPD, we can increase the efficiency of the upconversion detector to improve the secure key rate. Meanwhile, superconducting SPDs (SSPDs) have a higher detection efficiency and lower intrinsic dark count than upconversion SPDs. In our experiment, because of the limited space and tough environment in the container, we chose an upconversion SPD for its compact size and room-temperature operation. With future miniaturization of SSPDs, we can definitely improve the performance of the entire system. Moreover, for future satellite-to-ground communication with a very small zenith angle, Rayleigh scattering will dominate and we could have an even better SNR than in our ground experiment with 1,550 nm light.

Recently, a novel experiment[34] has been carried out that implements quantum state transfer from a GEO satellite to the ground and shows the potential of continuous variable QKD in daylight. Overall, compared with discrete-variable QKD, for example using a homodyne detector, continuous-variable QKD is more robust against background noise in daylight, but suffers from high channel losses[43,44].

Methods

Methods and any associated references are available in the online version of the paper.

Received 1 March 2017; accepted 8 June 2017;
published online 24 July 2017

References

1. Peng, C.-Z. *et al.* Experimental free-space distribution of entangled photon pairs over 13 km: towards satellite-based global quantum communication. *Phys. Rev. Lett.* **94,** 150501 (2005).
2. Schmitt-Manderbach, T. *et al.* Experimental demonstration of free-space decoy-state quantum key distribution over 144 km. *Phys. Rev. Lett.* **98,** 010504 (2007).
3. Jin, X.-M. *et al.* Experimental free-space quantum teleportation. *Nat. Photon.* **4,** 376–381 (2010).
4. Yin, J. *et al.* Quantum teleportation and entanglement distribution over 100-kilometre free-space channels. *Nature* **488,** 185–188 (2012).
5. Ma, X.-S. *et al.* Quantum teleportation over 143 kilometres using active feed-forward. *Nature* **489,** 269–273 (2012).
6. Wang, J.-Y. *et al.* Direct and full-scale experimental verifications towards ground-satellite quantum key distribution. *Nat. Photon.* **7,** 387–393 (2013).
7. Nauerth, S. *et al.* Air-to-ground quantum communication. *Nat. Photon.* **7,** 382–386 (2013).
8. Yin, J. *et al.* Experimental quasi-single-photon transmission from satellite to earth. *Opt. Express* **21,** 20032–20040 (2013).
9. Vallone, G. *et al.* Experimental satellite quantum communications. *Phys. Rev. Lett.* **115,** 040502 (2015).
10. Xin, H. Chinese academy takes space under its wing. *Science* **332,** 904–904 (2011).
11. Fritz, L. W. Commercial Earth observation satellites. *Int. Arch. Photogramm. Remote Sens.* **31,** 273–282 (1996).
12. Pratt, S. R., Raines, R., Fossa C. E. Jr & Temple, M. An operational and performance overview of the Iridium Low Earth Orbit satellite system. *IEEE Commun. Surv.* **2,** 2–10 (1999).
13. Gilmore, D. G. *Spacecraft Thermal Control Handbook: Fundamental Technologies* Vol. 1 (American Institute of Aeronautics and Astronautics, 2002).
14. Pfennigbauer, M., Leeb, W., Aspelmeyer, M., Jennewein, T. & Zeilinger, A. *Free-Space Optical Quantum Key Distribution Using Intersatellite Links* (CNES–Intersatellite Link Workshop, 2003).
15. Tomaello, A., Dall'Arche, A., Naletto, G. & Villoresi, P. Intersatellite quantum communication feasibility study. *Proc. SPIE* **8163,** 816309 (2011).
16. Buttler, W. T. *et al.* Daylight quantum key distribution over 1.6 km. *Phys. Rev. Lett.* **84,** 5652–5655 (2000).
17. Hughes, R. J., Nordholt, J. E., Derkacs, D. & Peterson, C. G. Practical free-space quantum key distribution over 10 km in daylight and at night. *New J. Phys.* **4,** 43 (2002).

18. Höckel, D., Koch, L., Martin, E. & Benson, O. Ultranarrow bandwidth spectral filtering for long-range free-space quantum key distribution at daytime. *Opt. Lett.* **34,** 3169–3171 (2009).
19. Restelli, A. *et al.* Improved timing resolution single-photon detectors in daytime free-space quantum key distribution with 1.25 GHz transmission rate. *IEEE J. Sel. Top. Quantum Electron.* **16,** 1084–1090 (2010).
20. Shan, X., Sun, X., Luo, J., Tan, Z. & Zhan, M. Free-space quantum key distribution with Rb vapor filters. *Appl. Phys. Lett.* **89,** 191121 (2006).
21. Rogers, D. *et al.* Free-space quantum cryptography in the H-alpha Fraunhofer window. *Proc. SPIE* **6304,** 630417 (2006).
22. Peloso, M. P., Gerhardt, I., Ho, C., Lamas-Linares, A. & Kurtsiefer, C. Daylight operation of a free space, entanglement-based quantum key distribution system. *New J. Phys.* **11,** 045007 (2009).
23. Miao, E.-L. *et al.* Background noise of satellite-to-ground quantum key distribution. *New J. Phys.* **7,** 215 (2005).
24. Shentu, G.-L. *et al.* Ultralow noise up-conversion detector and spectrometer for the telecom band. *Opt. Express* **21,** 13986–13991 (2013).
25. Ren, J.-G. *et al.* Long-distance quantum teleportation assisted with free-space entanglement distribution. *Chin. Phys. B* **18,** 3605 (2009).
26. Hwang, W.-Y. Quantum key distribution with high loss: toward global secure communication. *Phys. Rev. Lett.* **91,** 057901 (2003).
27. Wang, X.-B. Beating the photon-number-splitting attack in practical quantum cryptography. *Phys. Rev. Lett.* **94,** 230503 (2005).
28. Lo, H.-K., Ma, X. & Chen, K. Decoy state quantum key distribution. *Phys. Rev. Lett.* **94,** 230504 (2005).
29. Fung, C.-H. F., Ma, X. & Chau, H. F. Practical issues in quantum-key-distribution postprocessing. *Phys. Rev. A* **81,** 012318 (2010).
30. Huttner, B., Imoto, N., Gisin, N. & Mor, T. Quantum cryptography with coherent states. *Phys. Rev. A* **51,** 1863–1869 (1995).
31. Brassard, G., Lütkenhaus, N., Mor, T. & Sanders, B. C. Limitations on practical quantum cryptography. *Phys. Rev. Lett.* **85,** 1330–1333 (2000).
32. Lo, H.-K. & Preskill, J. Security of quantum key distribution using weak coherent states with nonrandom phases. *Quantum Inform. Comput.* **7,** 431–458 (2007).
33. Takenaka, H., Toyoshima, M. & Takayama, Y. Experimental verification of fiber-coupling efficiency for satellite-to-ground atmospheric laser downlinks. *Opt. Express* **20,** 15301–15308 (2012).
34. Günthner, K. *et al.* Quantum-limited measurements of optical signals from a geostationary satellite. *Optica* **4,** 611–616 (2017).
35. Lo, H.-K., Curty, M. & Qi, B. Measurement-device-independent quantum key distribution. *Phys. Rev. Lett.* **108,** 130503 (2012).
36. Braunstein, S. L. & Pirandola, S. Side-channel-free quantum key distribution. *Phys. Rev. Lett.* **108,** 130502 (2012).
37. Bennett, C. H. *et al.* Teleporting an unknown quantum state via dual classical and Einstein–Podolsky–Rosen channels. *Phys. Rev. Lett.* **70,** 1895–1899 (1993).
38. Briegel, H.-J., Dür, W., Cirac, J. I. & Zoller, P. Quantum repeaters: the role of imperfect local operations in quantum communication. *Phys. Rev. Lett.* **81,** 5932–5935 (1998).
39. Giovannetti, V., Lloyd, S. & Maccone, L. Quantum-enhanced measurements: beating the standard quantum limit. *Science* **306,** 1330–1336 (2004).
40. Yurke, B. Wideband photon counting and homodyne detection. *Phys. Rev. A* **32,** 311–323 (1985).
41. Komar, P. *et al.* A quantum network of clocks. *Nat. Phys.* **10,** 582–587 (2014).
42. Thew, R. T. *et al.* Low jitter up-conversion detectors for telecom wavelength GHz QKD. *New J. Phys.* **8,** 32 (2006).
43. Leverrier, A. Composable security proof for continuous-variable quantum key distribution with coherent states. *Phys. Rev. Lett.* **114,** 070501 (2015).
44. Jouguet, P. *et al.* Experimental demonstration of long-distance continuous-variable quantum key distribution. *Nat. Photon.* **7,** 378–381 (2013).

Acknowledgements

The authors thank Y.-A. Chen, Y. Cao, Y. Liu and Y. Xu for discussions. This work was supported by the National Fundamental Research Program (grant no. 2013CB336800), the 'Strategic Priority Research Program' of the Chinese Academy of Sciences (grant no. XDA04030000), the National Natural Science Foundation of China, the Chinese Academy of Sciences and the 10000-Plan of Shandong Province (Taishan Scholars).

Author contributions

Q.Z., C.-Z.P. and J.-W.P. conceived and designed the experiment. S.-K.L., J.L., W.C., Y.L., Z.-H.L., C.-Z.P. and J.-W.P. designed QKD devices. H.-L.Y., C.L., D.-D.L., B.L., H.D., Y.-H.G., J.-G.R., C.-Z.P. and J.-W.P. developed the SMF coupling technique. G.-L.S., J.-Y.G., J.S.P., M.M.F. and Q.Z. implemented upconversion detectors. S.-K.L., H.-L.Y., S.-Q.Z. and W.-Y.L. designed software. X.-B.W. contributed to the decoy-state analysis. Q.Z., C.-Z.P. and J.-W.P. analysed the data and wrote the manuscript, with input from S.-K.L., H.-L.Y. and C.L. All authors contributed to the data collection, discussed the results, and reviewed the manuscript. C.-Z.P. and J.-W.P. supervised the whole project.

Additional information

Supplementary information is available in the online version of the paper. Reprints and permissions information is available online at www.nature.com/reprints. Publisher's note: Springer Nature remains neutral with regard to jurisdictional claims in published maps and institutional affiliations. Correspondence and requests for materials should be addressed to Q.Z., C.-Z.P. and J.-W.P.

Competing financial interests

The authors declare no competing financial interests.

Methods

Alignment and calibration. A 500 mW, 532 nm beacon laser, coaxially located on the sending telescope, was pointed at the receiving site. We manually aligned the parabolic mirror to make sure that the green laser spot was pointed at the mirror's centre. A 2 W, 671 nm beacon laser, coaxially located on the receiving telescope, was pointed at the sending site. At the sending sites, a wide-field camera was installed behind the guide scope to take photographs of the red beacon light. This information was fed to the two-dimensional sending platform, which aligned the telescope to achieve optimal tracking of the 671 nm beacon light. This arrangement formed the coarse tracking system at the sending site. The fine tracking system consisted of a BS, an FSM, an interference filter (IF) and a complementary metal oxide semiconductor (CMOS) imaging sensor (Fig. 2). The BS was used to collect the 671 nm beacon light for fine tracking of the CMOS sensor, while the FSM was used to finely adjust the optical path according to a correction program using image information obtained by the fine-tracking CMOS imaging sensor.

At the sending site, as well as the 532 nm laser, we also used two additional lasers. One was a 10 mW, 810 nm beacon laser and the other a 1 W, 1,548 nm reference laser. The two lasers were mixed with signal light with a WDM and a BS, respectively (Fig. 2), and were used as beacon lights to align and track SMF coupling. At the receiving site, the SMF coupling system, mounted on a one-dimensional translation stage, consisted of an FSM, a DM and a CMOS. The FSM was just the secondary mirror of the receiving telescope, and the DM reflected telecom-band light and transmitted the 810 nm beacon light. The reflected telecom-band light was collimated into the SMF and the transmitted 810 nm light was captured by the CMOS imaging sensor. Before the QKD experiment, we combined a 810 nm laser and a 1,548 nm laser into a 3 m free-space collimator and shone the light to the receiving telescope to simulate the beacon light. With the simulated light, we first located the SMF in the focal point of the parabolic reflector by adjusting the translation stage, then aligned the FSM and DM to optimize the fibre coupling efficiency. Once the maximum efficiency was achieved, we recorded and marked the 810 nm light position by the CMOS sensor. During the QKD experiment, we first made sure that the 810 nm beacon light was located at the marked position of the CMOS imaging sensor, then we optimized the translation stage, the FSM and the DM by measuring the coupled optical power of the SMF with an InGaAs power meter. Meanwhile, a 850 nm beacon laser was also coupled into the fibre at the receiver side, working as a fine beacon for the transmitter.

In our experiment, the shift of the bandwidth of our lasers and detectors should be guaranteed. We used a high-precision optical spectrum analyser (OSA) at the source and detector. The OSA in Fig. 2a was for the source, and another was located at the input (Fig. 2e). The OSAs were self-calibrated in advance. After the link was established, a strong light (~1 W optical power) at 1,548 nm was sent from the transmitter to the receiver. With OSAs, the wavelength was precisely measured at the two terminals. The wavelength for the source and detector was calibrated with a precision smaller than 0.01 nm.

We adapted several lasers with different wavelengths (532, 671, 810, 850, 1,570, 1,548 and 1,550.14 nm) for various applications. The 1,550.14 nm wavelength is the wavelength for QKD. The 532, 671, 810 and 850 nm lasers are for coarse alignment, 1,548 nm for fine alignment and wavelength reference, and 1,570 nm for monitoring the link stability and channel losses. We needed to make sure that chromatic dispersion does not influence the system's performance. The 532 and 671 nm lasers were parallel to the optical link for the QKD and did not share the same optics as the signal, and the chromatic dispersion for them in the 53 km of air was negligible. The chromatic dispersion for the 1,548, 1,550.14 and 1,570 nm lasers was also negligible due to their small wavelength differences in relation to the QKD signal wavelength. So, only the 810 and 850 nm lasers were of concern. We used reflection optics instead of transmission optics as much as possible, as this can reduce chromatic dispersion. Moreover, the divergence angle for 810 and 850 nm was several times larger than the diffraction limit. In that sense, dispersion was not a problem for coarse alignment.

Data availability. The data that support the plots within this paper and other findings of this study are available from the corresponding authors upon reasonable request.